Molecular Crystals and Liquid Crystals Science and Technology. Section A. Molecular Crystals and Liquid Crystals

Publication details, including instructions for authors and subscription information:
http://www.tandfonline.com/loi/gmcl19

Lithium Transport Through Sputter Deposited Lithium Cobalt Dioxide Thin Film Electrode

Su-Il Pyun [a] & Heon-Cheol Shin [a]

[a] Department of Materials Science and Engineering, Korea Advanced Institute of Science and Technology, 373-1 Kusong-Dong, Yusong-Gu, Taejon, 305-701, KOREA

Version of record first published: 27 Oct 2006

To cite this article: Su-Il Pyun & Heon-Cheol Shin (2000): Lithium Transport Through Sputter Deposited Lithium Cobalt Dioxide Thin Film Electrode, Molecular Crystals and Liquid Crystals Science and Technology. Section A. Molecular Crystals and Liquid Crystals, 341:2, 147-154

To link to this article: http://dx.doi.org/10.1080/10587250008026132

Mol. Cryst. and Liq. Cryst., 2000, Vol. 341, pp. 147-154
Reprints available directly from the publisher
Photocopying permitted by license only

Lithium Transport Through Sputter Deposited Lithium Cobalt Dioxide Thin Film Electrode

SU-IL PYUN and HEON-CHEOL SHIN

Department of Materials Science and Engineering, Korea Advanced Institute of Science and Technology, 373–1 Kusong-Dong, Yusong-Gu, Taejon 305–701, KOREA

(In final form July 12, 1999)

Lithium transport through lithium cobalt dioxide thin film electrode prepared by rf-magnetron sputtering was investigated in 1M solution of $LiClO_4$ in propylene carbonate using cyclic voltammetry, galvanostatic intermittent titration technique (GITT) and potentiostatic current transient technique. The cathodic and anodic current transients exhibited the non-Fickian behaviour of lithium transport when the applied potential steps encountered potential plateaus near *3.91* $V_{Li/Li+}$, determined from GITT. It is suggested that the occurrence of this abnormal behaviour during lithium intercalation and deintercalation is accompanied by a 'diffusion-controlled' α/β phase transformation and 'cell-impedance-controlled' phase transformation, respectively. Lithium transport through the electrode comprising two phases of α and β has been theoretically considered by a numerical analysis of the phase transformation.

Keywords: lithium cobalt dioxide thin film; potentiostatic current transient; cell-impedance; phase transformation; numerical analysis

INTRODUCTION

Electrochemical lithium intercalation into and deintercalation from such transition metal oxides as $LiCoO_2$[1], $LiNiO_2$[2], $LiMn_2O_4$[3] etc., have been extensively studied by many researchers because of its importance as a cathode material in rechargeable lithium batteries.

Recently, we investigated lithium transport through carbon-dispersed composite electrodes of transition metal oxides such as $Li_\delta V_2O_5$ and $Li_{1-\delta}CoO_2$ by using current transient technique and reported that lithium transport showed the non-Fickian behaviour in the coexistence of Li-poor phase and Li-rich phase[4,5]. In addition, we have analysed the non-Fickian behaviour with respect

to the diffusion-controlled phase transformation using numerical method[6]. The electrochemical response obtained from the composite electrode, however, should be greatly distorted owing to the constituents of the composite electrode, *i.e.* organic binder and conductive additive[7]. So, it is necessitated to use binder- and carbon-free pure electrode for elucidation of lithium transport mechanism through the transition metal oxides.

In this respect, this work discusses lithium transport through the sputter deposited pure $Li_{1-\delta}CoO_2$ thin film electrode with respect to the phase transformation. For this purpose, cyclic voltammogram, open-circuit potential transients and cathodic/anodic current transients were measured on pure thin film electrode. Current transients have been simultaneously simulated as a function of lithium intercalation/deintercalation potential and compared with those experimentally measured.

EXPERIMENTAL

A $LiCoO_2$ disc (99.9% purity, 75 mm diameter, Kojundo Chem. Lab. Co., Ltd, JAPAN) and Ar gas (99.999% purity) were used as target material and sputter gas, respectively. $LiCoO_2$ film was deposited on 400 nm thick Pt current collector on alumina substrate at room temperature with an rf power of 200 W and an Ar gas pressure of 1.4 Pa by using a conventional rf-magnetron sputtering system (CemeCoat model CC300, Germany). The flow rate of Ar gas was adjusted by the mass flow control system (Sierra Instrument Model 202C-PE, U.S.A.).

After deposition, the electrode was heated in air at a rate of 5 °C min^{-1} and held at 700 °C for 4 h, then cooled at a rate of 2 °C min^{-1}. The thickness of the $LiCoO_2$ film was measured as a function of deposition time with alpha-step stylus (Tencor Instrument, U.S.A.). The average growth rate of the $LiCoO_2$ film was found to be 1.4 nm min^{-1}. The $LiCoO_2$ film electrode investigated in this work was deposited to a thickness ranging from 100 to 300 nm.

A three-electrode electrochemical cell was employed for the electrochemical measurements. The reference and counter electrodes were constructed from lithium foil (Foote Mineral Co. U.S.A., purity 99.9 %), and a 1 M $LiClO_4$ propylene carbonate (PC) solution was used as the electrolyte. The electrode area exposed to electrolyte amounted to 1 cm^2. All the electrochemical experiments were usually performed at 25 °C in a glove box (MECAPLEX GB94) filled with purified Ar gas.

Open circuit potential transients were obtained by charging/discharging the cell in steps of 0.5 μAh cm^{-2}. The charge/discharge current was selected so that a change in lithium content of $\Delta\delta = 1$ for $Li_{1-\delta}CoO_2$ would occur for 5 h. The deviation δ from the ideal stoichiometry of $LiCoO_2$ was estimated from the values of the mass of the oxide and of the total electrical charge that was transferred during the whole charge/discharge cycle.

The current transient experiment was performed by application of large potential steps *0.5* to *0.6 V*. Cathodic current transient was measured on the film electrodes with a thickness ranging from 100 to 300 nm by dropping *4.10* to *3.50* $V_{Li/Li+}$ and *4.00* to *3.50* $V_{Li/Li+}$. After measuring the cathodic current transient, the electrode potential was stepped from *3.50* $V_{Li/Li+}$ to the initial values *4.10* and *4.00* $V_{Li/Li+}$. From this moment on, the resulting anodic current transient was recorded with time.

RESULTS AND DISCUSSION

Figure 1 presents the cyclic voltammogram obtained from the $Li_{1-\delta}CoO_2$ thin film electrode with a thickness of 200 nm in 1M $LiClO_4$-PC solution at a scan rate of 1 mV s^{-1}. The cyclic voltammogram clearly showed three sets, *i.e.* the first set [3.94, 3.87], the second set [4.08, 4.06] and the third set [4.18, 4.16], of well-defined current peaks, indicating the highly crystallized structure of the $Li_{1-\delta}CoO_2$ film. The discrepancy between the anodic and cathodic peaks in each set is due to the internal resistance of the cell. The first set is attributed to lithium deintercalation from and intercalation into the intercalation sites in the oxide structure available for the lithium ion. The second and third sets are assigned to the order/disorder transition in the high temperature modification [8].

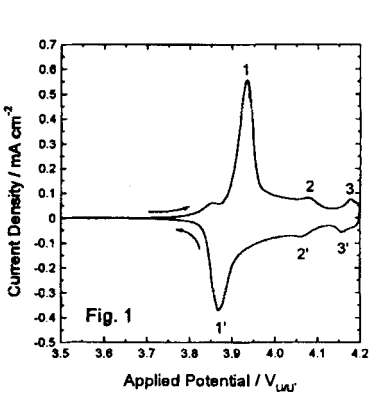

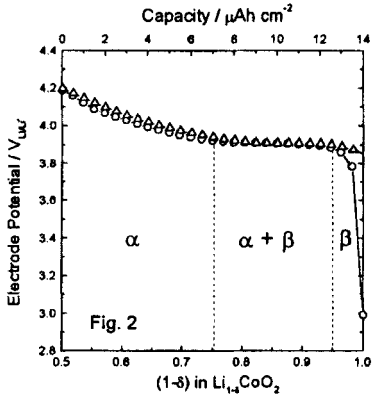

FIGURE 1 Cyclic voltammogram obtained from the $Li_{1-\delta}CoO_2$ thin film electrode with a thickness of 200 nm in 1M $LiClO_4$-PC solution at a scan rate of 1 mV s^{-1}.

FIGURE 2 Electrode potential obtained from the $Li_{1-\delta}CoO_2$ thin film electrode with a thickness of 200 nm in 1M $LiClO_4$-PC solution as a function of lithium content ($1-\delta$) during lithium intercalation (O) and deintercalation (Δ).

Figure 2 demonstrates electrode potential obtained from the first intermittent galvanostatic charge-discharge curve of the $Li_{1-\delta}CoO_2$ thin film electrode with a thickness of 200 nm in 1M $LiClO_4$-PC solution as a function of lithium content, $(1-\delta)$, ranging from 0.5 to 1.0. The electrode potential curve displayed a wide potential plateau near *3.91* $V_{Li/Li+}$ both during lithium intercalation and deintercalation in the $(1-\delta)$ range 0.75 to 0.95. The occurrence of the plateau is due to the coexistence of a Li-poor α phase and a Li-rich β phase. So, if the potential stepping passes through the plateau potential down/up towards the applied potential during the current transient experiment, lithium intercalates into the electrode comprising two phases of α and β.

Figure 3 illustrates on a logarithmic scale the cathodic current transients experimentally obtained with the $Li_{1-\delta}CoO_2$ thin film electrodes with a thickness ranging from 100 to 300 nm in a 1M $LiClO_4$-PC solution at two potential drops of *4.10* to *3.50* $V_{Li/Li+}$ and *4.00* to *3.50* $V_{Li/Li+}$. The current transient fell first in a slow upward convex shape, and then in an abrupt upward concave shape. In previous paper[6], we determined transition times $t_{tr(1)}$ and $t_{tr(2)}$ as the times of the local maxima on the derivatives of the linear and logarithmic current transients, respectively and asserted that these values of time correspond to the onset and end of the diffusion-controlled phase boundary movement, respectively. In this work, however, we do not obtain the low current level, so that we can not determine $t_{tr(2)}$. The value of $t_{tr(1)}$ is indicated on the respective current transient.

It should be noted that till $t=t_{tr(1)}$, the current transient does not follow the typical two-stage character of 'diffusion-controlled' lithium transport through the electrode subjected to potentiostatic boundary condition[9]. The ratio of the resulting initial current level (1.2×10^{-2} A) at one potential drop *4.10→3.50* $V_{Li/Li+}$ to the initial current level (1.0×10^{-2} A) at another potential drop *4.00→3.50* $V_{Li/Li+}$ is just identical to that ratio of one potential drop (0.60 V) to another potential drop (0.50 V). This means that current-potential relation follows Ohm's law. From this result, it seems reasonable to assume that lithium transport in the first stage is underlain by cell-impedance[10].

Now, let us theoretically consider the 'cell-impedance-governed' lithium transport. The initial condition (I.C.) and the impermeable boundary condition (B.C.) at the output side $x=L$ are given as

$$\text{I.C.}: \quad c = c_0 \qquad \text{for } 0 \le x \le L \text{ at } t = 0 \qquad (1)$$

$$\text{B.C.}: \quad -nF\bar{D}_{Li^+}(\partial c / \partial x) = 0 \qquad \text{for } x = L \text{ at } t > 0 \qquad (2),$$

where x is the distance into the electrode from the electrode/electrolyte interface; c, the local concentration of lithium ion; n, valence number; F, Faraday constant and $\bar{D}_{Li^+}$ represents the concentration-independent chemical diffusivity of lithium ion. In addition, the flux at the input side $x=0$ is determined by cell-impedance. The B.C. with respect to cell-impedance is expressed by

$$\text{B.C.}: \quad -nF\tilde{D}_{Li^+}(\partial c/\partial x) = (E - E_{app})/R \quad \text{for } x = 0 \text{ at } t > 0 \qquad (3),$$

where E is electrode potential; E_{app}, applied potential and R represents cell-impedance. The electrode potential E is given as a function of $(1-\delta)$.
The functional expression $E=f(1-\delta)$ was first obtained by polynomial regression analysis of the electrode potential curve in Fig. 2. Next we simulated the current transient for various electrode thicknesses under the assumption that lithium transport through the electrode is purely governed by cell-impedance. Figure 4 exhibits on a logarithmic scale the cathodic current transients determined from numerical solution to the Fick's diffusion equations for the conditions described above (Eqs. (1), (2) and (3)). The numerical current transient is divided into three stages of a slow upward convex-shaped decrease, an almost current plateau, and an exponential decay in sequence.

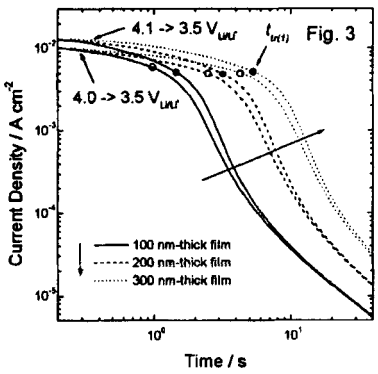

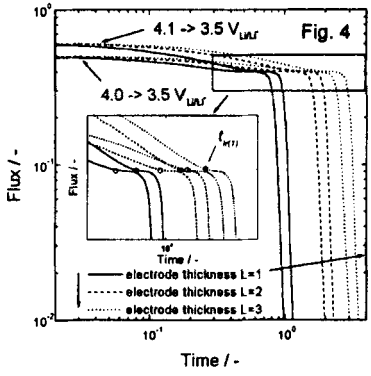

FIGURE 3 The cathodic current transients experimentally obtained from the $Li_{1-\delta}CoO_2$ thin film electrodes.

FIGURE 4 The cathodic current transients theoretically determined under the 'cell-impedance-controlled' constraint at the input side $x=0$ and impermeable boundary condition at the output side $x=L$, assuming $R=1$ and $nFD_{Li^+}=1$.

It is noticeable that the first stage of numerical current transient is similar to that first stage of experimental current transient in shape. From the measured levels of current transients, cell-impedance is estimated to be 45 to 50 $\Omega \cdot cm^2$, irrespective of the applied potential drops. On the other hand, the second stage of the numerical current transient, characterised by the current plateau, deviates strongly from that of the experimental current transient, characterised by the upward concave shape. In the previous work[6], it has been suggested that the upward concave shape characterises the 'diffuson-controlled' phase transformation by numerical analysis of current transient. From this result, it is

indicated that lithium transport through the electrode first in the single α phase range is purely governed by 'cell-impedance-controlled' constraint, which changes later in the coexistence of the two phases of α and β to 'diffusion-controlled' constraint.

This transition in lithium transport mechanism seems to be ascribed to the difference in the input flux between by chemical diffusion and by the quotient of potential drop divided by cell-impedance: the input flux given by $(E - E_{app}) / R$ is below the input flux given by $-\tilde{D}^{\alpha}_{Li^+}(\partial c / \partial x)_{x=0}$ into the electrode in the α phase range, thus 'cell-impedance-controlled' constraint becomes active to operate during lithium transport through the α phase. Since lithium ion has much lower chemical diffusivity in the β phase than in the α phase[11], the input flux of lithium $-\tilde{D}^{\beta}_{Li^+}(\partial c / \partial x)_{x=0}$ is much smaller than the input flux $-\tilde{D}^{\alpha}_{Li^+}(\partial c / \partial x)_{x=0}$. By contrast, the input flux $-\tilde{D}^{\beta}_{Li^+}(\partial c / \partial x)_{x=0}$ into the electrode in the β phase range is first exceeded by the input flux $(E - E_{app}) / R$, thus 'diffusion-controlled' constraint dominates lithium transport through the β phase.

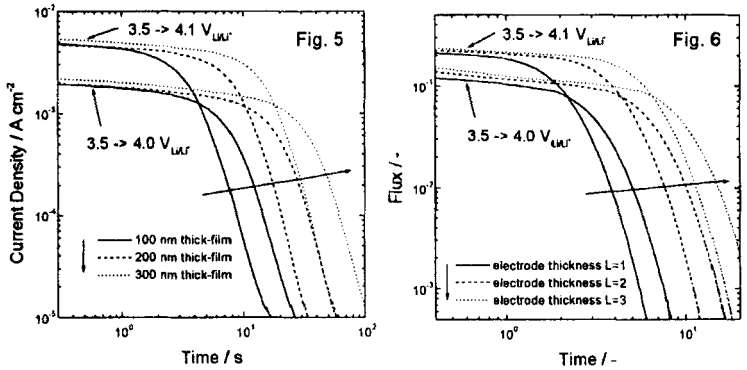

FIGURE 5 The anodic current transients experimentally obtained from the $Li_{1-\delta}CoO_2$ thin film electrodes.

FIGURE 6 The anodic current transients theoretically determined under the 'cell-impedance-controlled' constraint at the output side $x=0$ and impermeable boundary condition at the input side $x=L$, assuming $R=1$ and $nFD_{Li^+}=1$.

Figure 5 depicts on a logarithmic scale the anodic current transients experimentally obtained with the $Li_{1-\delta}CoO_2$ thin film electrode with a thickness ranging from 100 to 300 nm in a 1M $LiClO_4$-PC solution at two potential jumps

of *3.50* to *4.10* $V_{Li/Li+}$ and *3.50* to *4.00* $V_{Li/Li+}$. The current transient showed first an almost current plateau and then an exponential decay. Keeping in mind that the current plateau was observed during 'cell-impedance-controlled' phase transformation of α to β in the numerical current transient (Fig. 4) and the ratio of the resulting initial current level (4.7×10^{-3} A) at one potential jump *3.50→4.10* $V_{Li/Li+}$ to the initial current level (2.0×10^{-3} A) at another potential jump *3.50→4.00* $V_{Li/Li+}$ is just identical to that ratio of one potential difference (0.19 V) between the applied potential *4.10* $V_{Li/Li+}$ and the potential plateau *3.91* $V_{Li/Li+}$ to another potential difference (0.09 V) between the applied potential *4.00* $V_{Li/Li+}$ and the potential plateau, it seems reasonable to assume that lithium transport during deintercalation from the electrode is under the control of cell-impedance.

In view of these circumstances, we obtained the numerical solution for various electrode thicknesses under the 'cell-impedance-controlled' constraint (Eq. (3)) at the output side $x=0$ and impermeable boundary condition (Eq. (2)) at the input side $x=L$. The resulting anodic current transients are illustrated in Fig. 6 on a logarithmic scale. The simulated current transients (Fig. 6) shared almost exactly those experimental current transients (Fig. 5) in shape, indicating that phase transformation of β to α proceeds under the 'cell-impedance-controlled' constraint. This can be explained as follows. The output flux given by $(E - E_{app}) / R$ is first exceeded by the output flux given by $-\tilde{D}^{\alpha}_{Li^+}(\partial c / \partial x)_{x=0}$ from the electrode in the α phase range, thus 'cell-impedance-controlled' constraint becomes active to operate. Cell-impedance was determined from the measured levels of current transients to be *ca.* 45 to 50 $\Omega \cdot cm^2$, irrespective of the applied potential jumps.

CONCLUSIONS

In the present work, lithium transport through the sputter deposited pure $Li_{1-\delta}CoO_2$ thin film electrode has been discussed in view of phase transformation of Li-poor α phase to Li-rich β phase, and *vice versa*, leading to the following conclusions:

1. From the comparison of experimental current transient with theoretical current transient, it is suggested that lithium transport during intercalation into the electrode first in the single α phase range is purely governed by 'cell-impedance-controlled' constraint, which changes later in the coexistence of the two phases of α and β to 'diffusion-controlled' constraint. The transition in lithium transport mechanism can be accounted for as follows. The input flux by the quotient of potential drop divided by cell-impedance $(E - E_{app}) / R$ is first exceeded by the input flux by chemical diffusion $-\tilde{D}^{\alpha}_{Li^+}(\partial c / \partial x)_{x=0}$ in the single α phase range, whereas the input flux $-\tilde{D}^{\beta}_{Li^+}(\partial c / \partial x)_{x=0}$ is reached first in the coexistence of α and β.

2. Lithium transport during deintercalation from the $Li_{1-\delta}CoO_2$ film electrode in the coexistence of α and β is governed by cell-impedance. It is because the output flux $(E - E_{app})/R$ is first exceeded by the output flux $-\bar{D}^{\alpha}_{Li^+}(\partial c/\partial x)_{x=0}$ from the electrode during the whole lithium deintercalation time.

Acknowledgements

The authors are grateful to the Ministry of Commerce and Industry, Korea 1998/1999 and in part the KOSEF 1998/1999 through the CISEM at KAIST for financial support of this work.

References

[1] K. Mizushima, P. C. Jones, P. J. Wiseman, and J. B. Goodenough, *Mater. Res. Bull.* **15,** 783 (1980).
[2] J. R. Dahn, U. von Sacken, M. W. Juzkow, and H. Al-Janaby, *J. Electrochem. Soc.* **138,** 2207 (1991).
[3] M. M. Thackeray, P. J. Johnson, L. A. de Picciotto, P. G. Bruce, and J. B. Goodenough, *Mat. Res. Bull.* **19,** 179 (1984).
[4] J.-S. Bae, and S.-I. Pyun, *Electrochim. Acta* **90,** 251 (1996).
[5] Y.-M. Choi, S.-I. Pyun, and J. M. Paulsen, *Electrochim. Acta* **44,** 623 (1998).
[6] H.-C. Shin, and S.-I. Pyun, *Electrochim. Acta* **44,** 2235 (1999).
[7] I. Uchida, and H. Sato, *J. Electrochem. Soc.* **142,** L139 (1995).
[8] J. N. Reimers, and J. R. Dahn, *J. Electrochem. Soc.* **139,** 2091 (1992).
[9] C. John Wen, B. A. Boukamp, and R. A. Huggins, *J. Electrochem. Soc.* **126,** 2258 (1979).
[10] H.-C. Shin, and S.-I. Pyun, submitted to *Electrochim. Acta* for publication.
[11] Y.-M. Choi, S.-I. Pyun, J.-S. Bae, and S.-I. Moon, *J. Power Sources* **56,** 25 (1995).